

A conditional simulation of non-normal velocity/pressure fields

K.R. Gurley^{a,*}, A. Kareem^b

^a *Department of Civil Engineering, University of Florida, Gainesville, FL 32611, USA*

^b *Department of Civil Engineering and Geological Sciences, University of Notre Dame,
Notre Dame, IN 46556, USA*

Abstract

The simulation of random velocity and pressure signals at un-instrumented locations of a structure conditioned on measured records is often needed in wind engineering. Malfunctioning equipment may leave a hole in a wind data set or information may be lacking due to a limited number of instruments or difficulty in monitoring at certain locations. This paper presents a non-Gaussian conditional simulation technique in the context of non-Gaussian pressure fluctuations in separated flow regions, or velocity fluctuations in atmospheric flows. First, a uni-variate non-Gaussian simulation technique is developed. This is extended to multi-variate, and subsequently utilized as a mapping technique in a conditional simulation algorithm. This technique is applied to both the extension of existing records beyond recorded lengths, and the simulation of missing or damaged records based on measured data at other locations. © 1998 Published by Elsevier Science Ltd. All rights reserved.

1. Introduction

Simulation methods are becoming very attractive for the analysis and prediction of nonlinear system response as computational expense decreases with increasing computer hardware speed. Implementation of time domain methods require simulated load time histories with specific statistical and spectral characteristics. Many of the studies encompassing analysis and modeling of wind effects on structures have tacitly assumed that the involved random processes are Gaussian. This assumption is valid for integrated load effects of the random pressure field over large areas. However, regions under separated flows experience strong non-Gaussian effects in the pressure distribution characterized by high skewness and kurtosis, and may be highly

*Corresponding author.

correlated over the entire separation region. The non-Gaussian pressure effects lead to non-Gaussian local loads, and result in increased expected damage in glass panels and higher fatigue effects on other components of cladding. When the assumption of Gaussian wind loading is inappropriate, techniques for simulating non-Gaussian loading must be sought. This work introduces multi-variate non-Gaussian conditional simulation methods capable of producing realizations with a wide range of spectral and probabilistic characteristics conditional on measured records at some locations. The correlation between multiple locations is accurately simulated, while maintaining the appropriate spectral and probabilistic content of the processes at each location.

2. Background: modified Hermite transformation

An earlier study [1] presents the development of the so-called forward and backward modified Hermite transformations. Forward transformation produces a non-Gaussian process, x , through static transformation of a Gaussian process, u , using [2]

$$x = u + d_3(u^2 - 1) + d_4(u^3 - 3u). \quad (1)$$

The forward modified Hermite transform identifies the optimum values for the polynomial coefficients d_3 and d_4 such that x matches the desired values of skewness and kurtosis. The backward modified Hermite transform identifies the appropriate coefficients in the inverse of Eq. (1) necessary to produce a Gaussian process, u , from a non-Gaussian process, x . The forward and backward modified Hermite transformations are applied in a non-Gaussian simulation algorithm in the next section.

3. Spectral correction: A non-Gaussian simulation technique

Spectral correction is a robust new non-Gaussian simulation method which utilizes user specified non-Gaussian characteristics and frequency content in the form of target moments through fourth order and a target power spectrum. Alternatively, the user may define non-Gaussian characteristics through a marginal PDF model. A schematic of the method is shown in Fig. 1. An iterative application of corrective transformations provides convergence to the desired spectral and probabilistic characteristics.

Following from the top left in the schematic, the target spectrum G^T is applied to produce a Gaussian process u using a standard Gaussian simulation routine [3,4]. u is sent through a moment correction transformation, consisting of a forward modified Hermite transformation to yield a process x which matches the desired skewness and kurtosis ($u \rightarrow x$). This non-Gaussian process x has a power spectrum G^x which no longer matches the target spectrum G^T due to distortions in the transformation. The process x is sent through a spectral correction to produce x_c which fits the target spectrum G^T , and maintains the phase in x ($x \rightarrow x_c$). The distorted skewness and

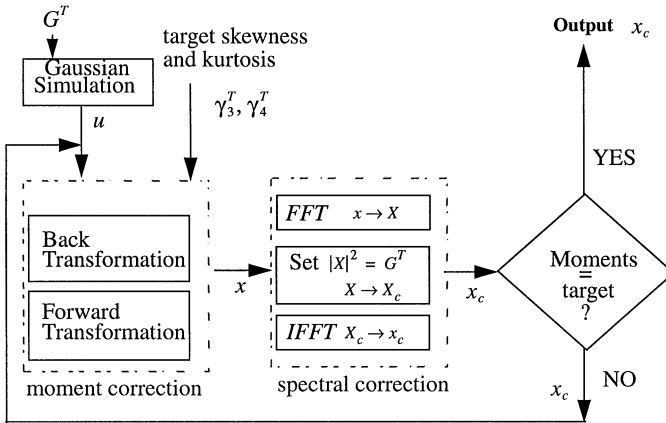


Fig. 1. Schematic of the spectral correction non-Gaussian simulation method.

kurtosis of x_c are compared with the target values using

$$\text{err} = |(\gamma_3^T - \gamma_3)/\gamma_3^T| + |(\gamma_4^T - \gamma_4)/\gamma_4^T|, \tag{2}$$

where γ_3^T, γ_4^T are the target, and γ_3, γ_4 are the measured skewness and kurtosis from x_c . If the error, err, is unacceptably large, the second iteration begins by sending the process with the correct spectrum and distorted skewness and kurtosis, x_c , back to the top of the loop to the moment correction. Here the skewness and kurtosis are again corrected using the backward and then forward modified Hermite transform to produce the second iteration of x ($x_c \rightarrow x_2$). The iterations continue, checking the error, err, after each spectral correction transformation, until the distorted moments of x_c converge to the target moments within a set tolerance. The spectrum of the resulting simulated process matches the target, and the skewness and kurtosis will be within user-specified tolerance. Typically, two or three iterations are required for convergence [5].

The modified Hermite transform may be replaced with a CDF-type mapping when the marginal PDF model associated with the modified Hermite transform is inappropriate [6]. This provides the option of describing the non-Gaussian characteristics of the desired process with either the first four moments, or a marginal PDF model.

3.1. Example: simulated non-Gaussian suction pressure on a rooftop

This example uses full-scale pressure data measured on the roof of an instrumented building at Texas Tech University. The spectral correction algorithm is used to simulate measured samples of pressure data in a separated flow region. The left side of Fig. 2 shows a comparison of the measured data sample and a single simulation realization. The realization is generated using a target spectrum estimated from the data and the first four measured moments. Note the similarities between measured and simulated samples including strong negative skewness, dominant low-frequency

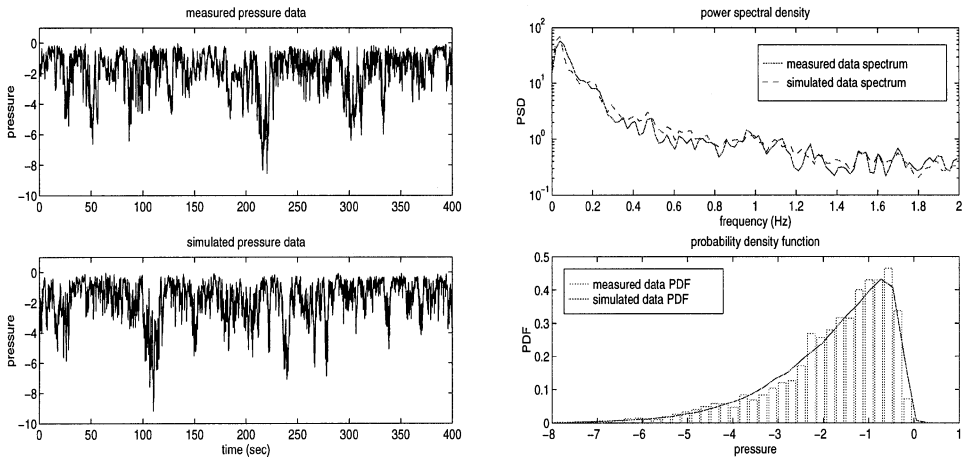


Fig. 2. Left: measured and simulated pressure data. Right: power spectral density and probability density function of measured and simulated pressure data.

content, frequently clustered extreme peaks, and a zero rate of crossing into positive pressure. Similarities are also observed through comparisons of the power spectral density and probability density function estimated from the measured data and simulated data in the right side of Fig. 2. The spectral correction simulation method closely emulates these important characteristics in the measured non-Gaussian data.

4. Multivariate spectral correction

Spectral correction is extended to simulate multiple correlated non-Gaussian time histories. Multivariate simulation becomes necessary for cases where non-Gaussian processes at spatially distributed locations are desired. For example, simulation of pressure along the roof edge or along the corner region of a building, where pressure under separated flow can be well correlated across the entire length.

The univariate algorithm in the previous section begins with a single Gaussian simulation, and iteratively corrects the power spectrum and PDF of the simulated realization. The multivariate spectral correction simulation algorithm starts with a multivariate Gaussian simulation, applies iterative corrections to the power spectrum and PDF of each process, and additionally updates the cross-spectrum used to simulate the initial Gaussian processes. The iterative corrections to the cross-spectrum result in a convergence to the desired correlation between the resulting simulated non-Gaussian processes.

The correlation updating scheme operates on the inverse Fourier transform of the cross-spectrum, the cross-correlation function, $R_{ij}^D(\tau)$. Pairs of simulated processes whose cross-correlation matches the target, $R_{ij}^{Nc}(\tau) = R_{ij}^T(\tau)$, will reflect the desired linear correlation between the i th and j th processes.

A schematic representation of the multivariate simulation algorithm is given in Fig. 3. Beginning at the top left, the target autospectrum, G_{ii}^T , and target skewness and kurtosis, γ_3^T, γ_4^T , of each process is input to the algorithm, along with the target cross-correlation function between each pair of processes, R_{ij}^T . A standard multivariate Gaussian simulation algorithm [7,8] produces a set of Gaussian processes with the design cross-correlation function, R_{ij}^D , and target auto-spectrum, G_{ii}^T . This design cross-correlation is initially set to the target cross-correlation function for the first iteration ($R_{ij}^D = R_{ij}^T$). Each Gaussian process is then transformed to non-Gaussian using spectral correction ($x_G^i \rightarrow x_{NG}^i$). The cross-correlation between these non-Gaussian processes are measured, $R_{ij}^{x_{NG}}$, and compared with the target values, R_{ij}^T . If the error is too large, a second iteration is begun, otherwise the set of processes x_{NG}^i are accepted as the output. Two or three iterations provides convergence to the target cross-correlation function.

At the end of an iteration, the design cross-correlation function is updated for the next iteration using

$$R_{ij}^D(it + 1) = \left(\rho_{ij}^D(it) + \frac{|\rho_{ij}^D(it)|[\rho_{ij}^T - \rho_{ij}^{x_{NG}}(it)]}{\max(|\rho_{ij}^D(it)|)} \right) (\max(|R_{ij}^T|)) \quad \text{over all } \tau, \quad (3)$$

using the following, with the function of iteration notation (it) replaced by the function of time lag (τ) notation:

$$\begin{aligned} \rho_{ij}^D(\tau) &= (R_{ij}^D(\tau))/(\max(|R_{ij}^T(\tau)|)), & \rho_{ij}^T(\tau) &= (R_{ij}^T(\tau))/(\max(|R_{ij}^T(\tau)|)), \\ \rho_{ij}^{x_{NG}}(\tau) &= (R_{ij}^{x_{NG}}(\tau))/(\max(|R_{ij}^T(\tau)|)). \end{aligned} \quad (4)$$

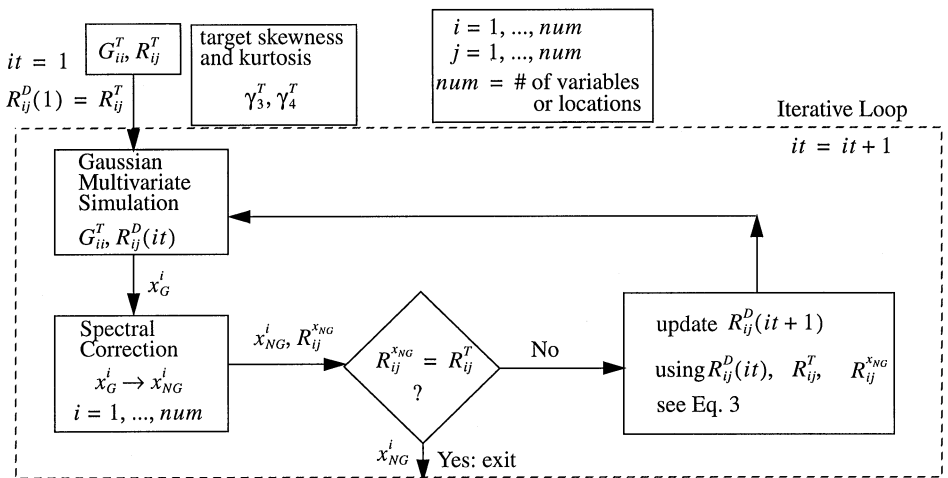


Fig. 3. Schematic of the multivariate spectral correction simulation method.

4.1. Example: rooftop pressure at three locations

This example again uses the full-scale pressure data, measured simultaneously at several locations on the roof of an instrumented building. We consider three locations on the roof in a separation zone where the pressure is highly non-Gaussian. The goal

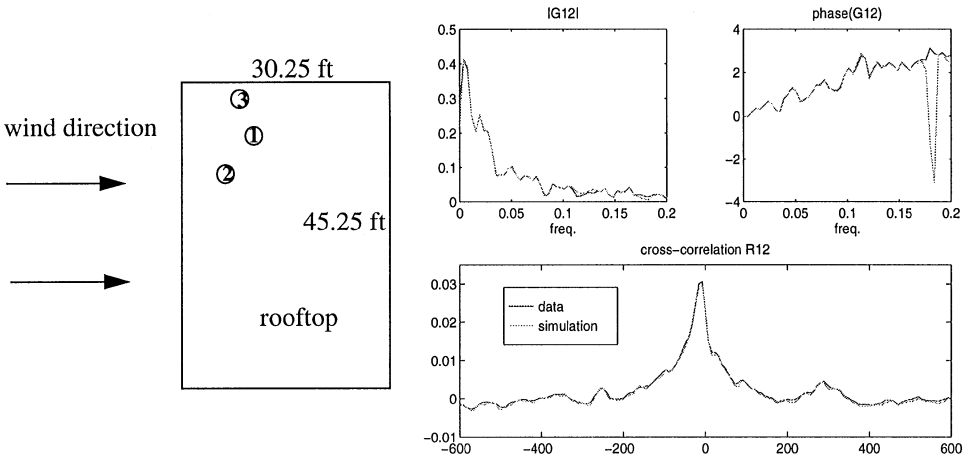


Fig. 4. Left: location of pressure taps. Right: comparisons of measured and simulated correlation statistics. Top left: absolute value of the cross-spectrum between locations 1 and 2; top right: phase of the cross-spectrum between locations 1 and 2; bottom: cross-correlation function.

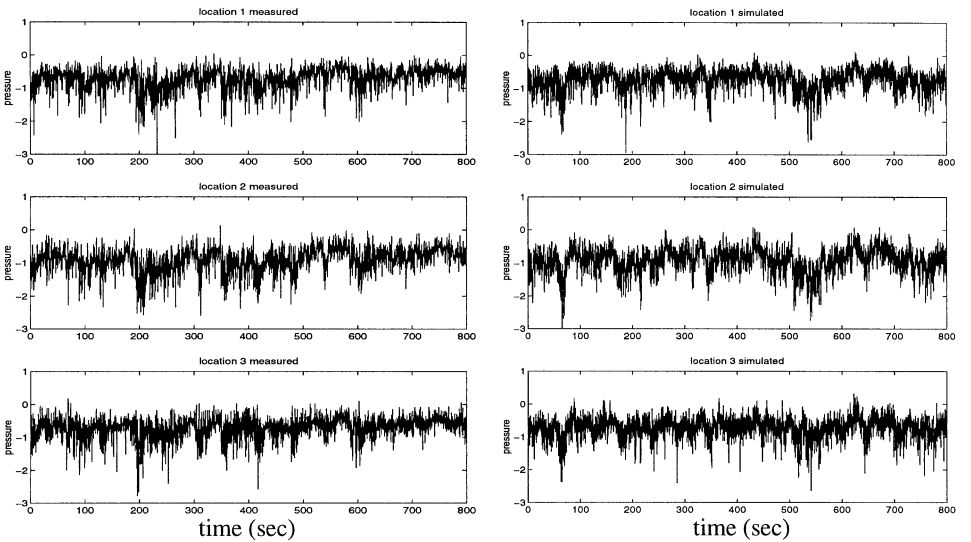


Fig. 5. Left: measured rooftop pressure at the three locations in Fig. 4. Right: simulated rooftop pressure at the three locations in Fig. 4.

is to generate realizations of three pressure records which maintain the measured cross-spectral density, and properly reflect the higher-order statistics and spectral contents at each location. Fig. 4 is a diagram of the approximate locations of the pressure taps. The offset leads to a non-zero phase relationship between locations. Fig. 4 also compares the target and simulated cross-spectral density function and cross-correlation between locations 1 and 2. The match between target and simulated cross-spectra is excellent. Fig. 5 shows the three measured pressure records, and their simulations using non-Gaussian multi-variate spectral correction. The low frequency correlation can be seen in both figures, along with the distinct non-Gaussian characteristics of the measured and simulated records.

5. Non-Gaussian conditional simulation

The formulation for Gaussian conditional simulation is first presented. Extensions are then made to non-Gaussian conditional simulation using the spectral correction algorithm.

5.1. Gaussian conditional simulation

Consider a pair of correlated Gaussian random vectors V_k and V_u . Let the two variate normal distribution of these variables be denoted

$$p(V) = p \begin{bmatrix} V_k \\ V_u \end{bmatrix} = N \left(\begin{bmatrix} \mu_k \\ \mu_u \end{bmatrix}, \begin{bmatrix} C_{kk} & C_{ku} \\ C_{uk} & C_{uu} \end{bmatrix} \right), \quad (5)$$

where μ_i is the mean value of the variable i , and C_{ij} is the cross-covariance between the variables i and j . If a sample of V_k is measured and denoted as v_k , then it is the conditional simulation of V_u based on the measured record v_k that is desired. This problem has been addressed in several forms [9–12], each of which leads to an equivalent final form for the conditional PDF of V_u given the information on V_k :

$$p(V_u | V_k = v_k) = N(\mu_u + C_{ku}^T C_{kk}^{-1}(v_k - \mu_k), C_{uu} - C_{ku}^T C_{kk}^{-1} C_{ku}). \quad (6)$$

A conditional simulation is then provided by [9,10,12]

$$(V_u | V_k = v_k) = C_{ku}^T C_{kk}^{-1}(v_k - V_k) + V_u, \quad (7)$$

where V_k , V_u are unconditionally simulated variates, and v_k is the known measured variate. Derivations of the covariance matrices C_{kk} and C_{ku} provide the information needed for Gaussian conditional simulation.

5.2. Frequency domain Gaussian conditional simulation

Frequency domain conditional simulation is applicable for generating realizations of time series at unmeasured locations n, \dots, N based on measured records at other

spatial locations $1, \dots, n-1$. It is assumed that the spectral density matrix between the $n-1$ known and the $N-n+1$ unknown locations is available.

The covariance matrices C_{kk} and C_{ku} are represented in the frequency domain as

$$C_{kk} = \begin{bmatrix} G_{11} & G_{12} & \cdots & G_{1,n-1} \\ G_{21} & G_{22} & \cdots & G_{2,n-1} \\ \vdots & \vdots & \vdots & \vdots \\ G_{n-1,1} & G_{n-1,2} & \cdots & G_{n-1,n-1} \end{bmatrix},$$

$$C_{ku} = \begin{bmatrix} G_{1,n} & G_{1,n+1} & \cdots & G_{1,N} \\ G_{2,n} & G_{2,n+1} & \cdots & G_{2,N} \\ \vdots & \vdots & \vdots & \vdots \\ G_{n-1,n} & G_{n-1,n+1} & \cdots & G_{n-1,N} \end{bmatrix}. \quad (8)$$

The sub-matrices in Eq. (8) are composed of elements of the cross-spectral matrix between locations i and j .

5.3. Time domain Gaussian conditional simulation

The conditional simulation in the time domain is applied to extend the length of a measured process. The measured realization $v_k(t)$ consists of discrete time components $t = 1, \dots, n-1$, and the unknown realization $v_u(t)$ is a continuation of the known realization over time $t = n, \dots, N$. The simulated realizations V_k, V_u in Eq. (7) now consist of a simulation $v(1 \dots N)$ based on the measured realization $v_k(1, \dots, n-1)$ that extends to time $t = N$. This single simulated realization is partitioned into the known and unknown portions:

$$v(1, \dots, N) = [v_k(1, \dots, n-1) (V_u(n, \dots, N) | V_k = v_k)]. \quad (9)$$

The covariance matrix in Eq. (7) consists of elements from the covariance vector

$$C_{kk} = \begin{bmatrix} c_0 & c_1 & c_2 & \cdots & c_{n-1} \\ c_1 & c_0 & c_1 & \cdots & c_{n-2} \\ \vdots & \vdots & \vdots & \vdots & \vdots \\ c_{n-1} & c_{n-2} & c_{n-3} & \cdots & c_0 \end{bmatrix},$$

$$C_{ku} = \begin{bmatrix} c_n & c_{n+1} & c_{n+2} & \cdots & c_N \\ c_{n-1} & c_n & c_{n+1} & \cdots & c_{N-1} \\ \vdots & \vdots & \vdots & \vdots & \vdots \\ c_1 & c_2 & c_3 & \cdots & c_{N-n+1} \end{bmatrix}, \quad (10)$$

where c_i are elements of the cross-covariance vector from either the Fourier transform of the measured power spectrum or a temporal calculation.

5.4. Extension to non-Gaussian conditional simulation

The conditional simulation using Eq. (7) requires that the variates V_k, V_u, v_k be Gaussian. The conditionally simulated variate V_u will then also be Gaussian. In order to conditionally simulate non-Gaussian records, Eq. (7) is applied to an initial set of Gaussian processes, and the result is mapped into the desired non-Gaussian domain, using spectral correction. The correlation between the simulation at the unknown location and the measured records at other locations is used to iteratively update the cross-correlation matrix used to generate the initial set of Gaussian processes. A previous non-Gaussian conditional simulation algorithm [13] uses correlation distortion based transformations for the mapping, and is thus limited to simulation of wide-banded processes. The use of spectral correction here is appropriate for wide-banded processes, and additionally permits the conditional simulation of more narrow-banded processes.

Fig. 6 is a schematic of the non-Gaussian frequency domain conditional simulation algorithm. The algorithm begins with the known non-Gaussian processes v_k , the measured covariance matrix C_{kk} , the target spectra of the unknown processes G_{uu}^T , the target skewness and kurtosis γ_3^T, γ_4^T , and the target cross-covariance matrix between the known and unknown processes C_{ku}^T . The design cross-covariance is set to the target cross-covariance $C_{ku}^D = C_{ku}^T$ for the first iteration. Gaussian simulations of V_k, V_u denoted V_k^G, V_u^G are generated using the input $C_{kk}, C_{ku}^D, G_{uu}^T$, and a standard multivariate Gaussian simulation algorithm. A modified Hermite transform is applied to v_k to produce a Gaussian variate v_k^G . Eq. (7) is then applied to produce a Gaussian conditional simulation at the unknown locations, denoted v_u^G . The Gaussian process, v_u^G , is sent through the Spectral Correction transformation to produce the

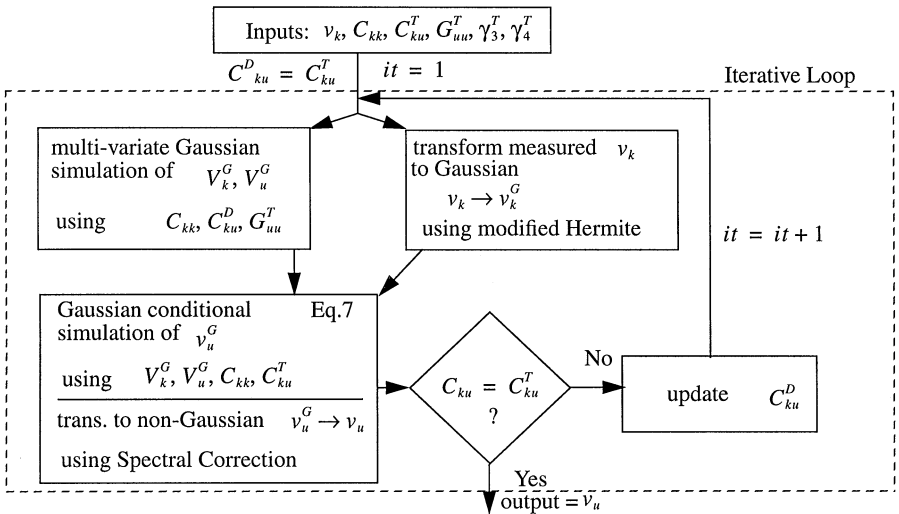


Fig. 6. Schematic of the conditional simulation algorithm using spectral correction.

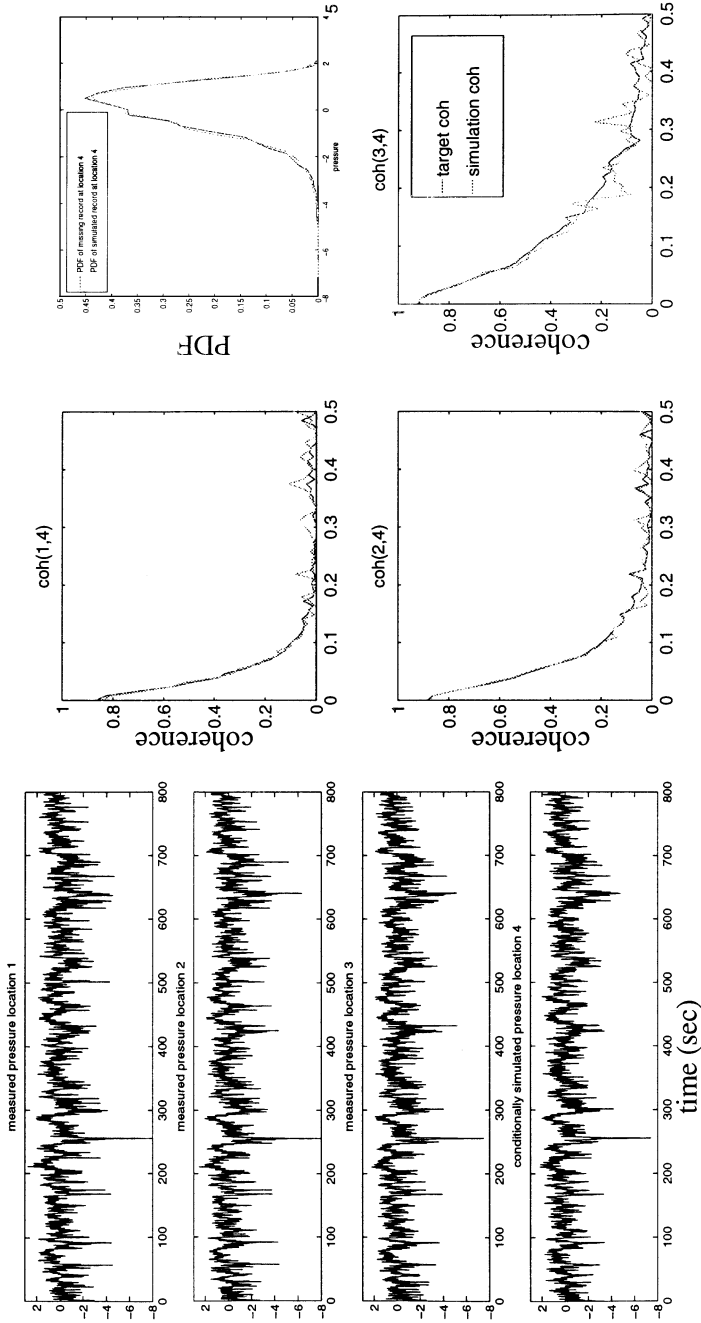


Fig. 7. Left: three known pressure records and a conditionally simulated record at location 4. Right: comparison of the target and simulated coherence functions between the simulated and measured locations. Top right: PDF of the pressure record at location 4 that is assumed missing (denoted measured), and histogram of its replacement using non-Gaussian conditional simulation.

non-Gaussian simulation v_u with target skewness and kurtosis, and autospectra G_{uu}^T . The cross-covariance, C_{ku} , between v_k and v_u are measured and compared with the target cross-covariance C_{ku}^T . If the error between the measured and target covariance is not acceptable, the design cross-covariance, C_{ku}^D , used to generate V_k^G , V_u^G is updated for use in the next iteration.

5.5. Example: simulation of pressure on building rooftop at a fourth locations using three measured locations

The statistics of measured non-Gaussian roof suction pressure records are used in conjunction with a standard wind velocity coherence model to generate four spatially separated non-Gaussian pressure records. The locations are assumed to be 4 m apart perpendicular to the wind direction, and no separation parallel to the wind direction. The skewness and kurtosis of each process is $-1.05, 5.5$, respectively. The fourth location is assumed to be damaged, and the conditional simulation algorithm presented above is used to replace it based on knowledge of the other three records.

The left side of Fig. 7 is a view of the three known records and the simulated fourth record. Note the strong low-frequency correlation among all four records. The right side of Fig. 7 shows the target and measured coherence between locations 1 and 4, 2 and 4, and 3 and 4. The match demonstrates that the simulation is a suitable replacement for the missing record. The far right top plot in Fig. 7 is a comparison of the PDF of the missing recorded and its replacement. The use of spectral correction in the conditional simulation algorithm ensures excellent agreement between target and simulated marginal distribution and autospectrum.

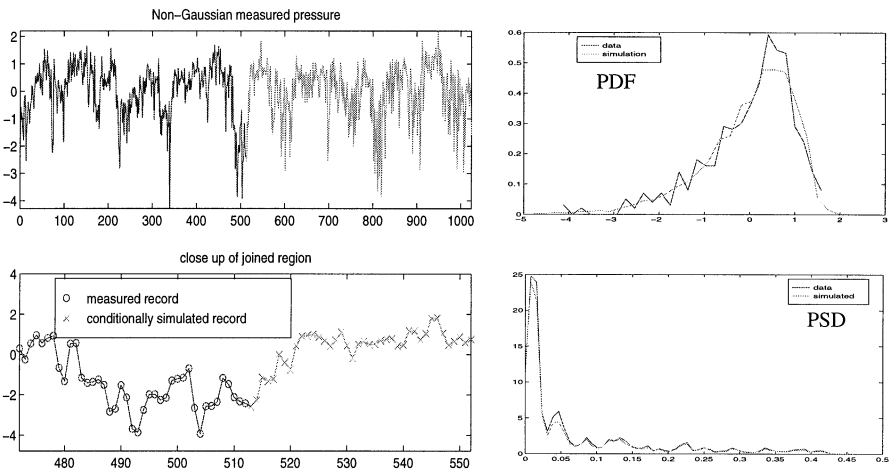


Fig. 8. Left: measured rooftop pressure data and a non-Gaussian conditional simulation. Right: PDF and PSD of measured and full extended pressure record.

5.6. Example: extension of a single non-Gaussian pressure record

An example of the time domain non-Gaussian conditional simulation method is shown in Fig. 8, where the measured rooftop suction pressure is conditionally simulated. The measured data consists of $\tau = 512$ points, and the total desired length is $T = 1024$ points. A close up of the joining region is shown to demonstrate smooth transition from measured to simulated data. The upper right plot shows good comparison between the measured and extended marginal PDF, and the lower right plot compares the PSD of the measured and extended records. This example demonstrates the applicability of the time domain non-Gaussian conditional simulation algorithm to extend existing records while maintaining spectral and probabilistic characteristics.

6. Conclusions

The non-Gaussian multivariate and conditional spectral correction simulation algorithms are shown to be effective for generating realizations of time histories, at one or more spatial locations, which match target characteristics given in the form of an autospectrum, a marginal probability density function, and cross-correlation functions between multiple processes. Spectral correction is extended to the conditional simulation of non-Gaussian processes to replace missing or damaged records. These algorithms provide additional tools for generating input to Monte Carlo-based simulation methods of structural reliability analysis, particularly for cases where environmental loading differs significantly from Gaussian.

Acknowledgements

The support for this work was provided in part by NSF Grants CMS9402196, and CMS95-03779, ONR Grant N00014-93-1-0761, and a grant from Lockheed-Martin. The first author was partially supported by a Department of Education GAANNP Fellowship during this study. Experimental data was kindly provided by Texas Tech University.

References

- [1] K. Gurley, A. Kareem, M. Tognarelli, Simulation of a class of non-Normal random processes, *Int. J. Non-Linear Mech.* 31 (5) (1996) 601–617.
- [2] S.R. Winterstein, Nonlinear vibration models for extremes and fatigue, *J. Eng. Mech. ASCE* 114 (10) (1988) 1772–1790.
- [3] M. Grigoriu, On the spectral representation method in simulation, *Prob. Eng. Mech.* 8 (1993) 75–90.
- [4] M. Shinozuka, C.M. Jan, Digital simulation of random processes and its applications, *J. Sound Vib.* 25 (1) (1972) 111–128.
- [5] K. Gurley, A. Kareem, Analysis, interpretation, modelling and simulation of unsteady wind and pressure data, *J. Wind Eng. Ind. Aerodyn.* 69–71 (1997) 657–669.

- [6] M. Grigoriu, Crossing of non-Gaussian translation processes, *J. Eng. Mech. ASCE* 110 (EM4) (1984) 610–620.
- [7] M. Shinozuka, Simulation of multivariate and multidimensional random processes, *J. Acoust. Soc. Am.* 49 (1971) 357–368.
- [8] L.E. Wittig, A.K. Sinha, Simulation of multicorrelated random processes using the FFT algorithm, *J. Acoust. Soc. Am.* 58 (3) (1975) 630–634.
- [9] L.E. Borgman, *Irregular Ocean Waves: Kinematics and Forces*. The Sea, Prentice-Hall, Englewood Cliffs, NJ, 1990.
- [10] M. Hoshiya, Kriging and conditional simulation of a Gaussian field, *J. Eng. Mech. ASCE* 121 (2) (1995) 181–186.
- [11] H. Kameda, H. Morikawa, An interpolating stochastic process for simulation of conditional random fields, *Probab. Eng. Mech.* 7 (4) (1992) 242–254.
- [12] D.G. Krige, Two-dimensional weighted moving average trend surfaces for ore evaluation, *J. South African Inst. of Mining and Metallurgy, Proc. Symp. on Mathematical Statistics and Computer Applications for Ore Evaluation*, Johannesburg, South Africa, 1966, pp. 13–38.
- [13] I. Elishakoff, Y.J. Ren, M. Shinozuka, Conditional simulation of non-Gaussian random fields, *Eng. Struct.* 16 (7) (1994) 558–563.